"Identification of Lithology and Structures in Serdo, Afar, Ethiopia Using Remote Sensing and Gis Techniques"

Addis Seid[1], T. Suryanarayana[2]

[1]College of Natural Science, Department of Geology, Wollo University, Dessie Campus, Ethiopia.
[2] College of Natural Science, Department of Geology, Wollo University, Dessie Campus, Ethiopia.

ABSTRACT: *New generations of advanced remote sensing data have been used by Earth scientists over the last decades. This study presents the applicability of recently launched Landsat 8 and Shuttle Radar Topographic Mission digital elevation model data for lithology and structure mapping. Processing of multispectral medium resolution of landsat8 and digital elevation model data were used for detection and mapping lithology and structure in the Serdo area. These data have been processed and interpreted with the production of lithologic and structural maps at a scale of 1:100,000. The results revealed that lithologic features and their textural characteristics are easily identified by coastal/aerosol, visible, near-infrared, and short-wave infrared (1-7) bands with resolution merge of band 8 (pan) bands. Spatial enhancement of landsat8 data using convolution filters (the spatial domain of the image) and digital elevation model (DEM) extracted from the SRTM have been used for structures extraction. Hill-shading techniques are applied to SRTM DEMs to enhance terrain perspective views and to extract morphologically defined structures. Faults and a different set of fracture systems are major structural elements recognized. Six main lithologic types and 1859 structures are identified, and totally12321 km² area was mapped in this work.*

Keywords: *Landsat8, lithology, DEM, NIR, Structures, Spatial Enhancement.*

I. INTRODUCTION

A. Background of the Study

Mapping lithology and structures require cumbersome fieldwork investigations. However, fieldwork is usually time-consuming and may take up years to complete, depending primarily on the extension and/or the accessibility of the area under investigation. Multispectral satellite remote sensing technology provides a relatively efficient and low-cost method for the geological mapping of terrains that are geologically complex or poorly or expensively accessible. Remote sensing data, such as aerial photographs and multispectral imagery data, can provide more continuous and detailed information, and quantitative interpretations can be made for large areas, thus enabling even the most inaccessible terrain to be mapped. However, the results of digital image processing and analysis require a field investigation in some selected testing areas in order to estimate the accuracy of the geological interpretation. According to Drury (1987), remote sensing has the advantage of providing synoptic overviews of the region; thus, it may directly pinpoint the characteristics of structures and geological features extending over large areas. As opposed to fieldwork investigations, remote sensing, along with image processing techniques, accounts for a less time-consuming and more cost-effective method for lithology and structure investigation. Nonetheless, such techniques in no way replace field investigations, but on the contrary, they complement each other. According to Laake (2011), using Landsat multi-band RGB (7,4,2) clearly distinguished between the basement rocks, the Mesozoic clastic sedimentary rocks, and coastal carbonates, while the difference between bands 4 and 2 highlighted a difference in lithology between pure limestone and more sand cover. The use of transformed data space using methods such as PCA and ICA helps to decorrelate band information while separating data along new component lines, which can further be enhanced by visualizing the new components in FCC.

B. Problem of Statement

Since Remote sensing and geographic information, the system is acquiring information without any physical contact and analyzing gathered data to provide meaningful full scene using a human skull with the aid of a device called a computer and different software.

In Ethiopian borders, desert, and semi-desert areas, the local geology is still unstudied at large scale due to many challenging factors such as economy, the climate of an area, inaccessibility of the area, and security problems; especially the latter two factors are very common in Afar and Regional Somali states. So, this research is designed to study and provide up-to-date and qualified geosciences information for the country's development by assessing the areas which are more challenged through remote sensing and Geographic Information System method and techniques in Afar Region, Serdo area Ethiopia.

C. Local Geology

Afar rift is the most active segment of the entire East African Rift System (EARS), with Erta Ale volcano being presently active. Studies by Mohr (1972) indicate that over 90% of the eruptives are of silicic composition. The Afar rift floor is dotted with a large number of rhyolitic volcanoes in the south and more basaltic centers in the north. The surface geology in the south is similar to that of the MER, where ignimbrites are abundant, while in the north, basalt sheets of Quaternary age dominate. The volcanic overlie older sedimentary rocks in the Afar rift zone. The Afar depression of Ethiopia is a significant area of graben fracturing showing all tectonic and volcanic consequences. It is a part of the afro-Arabian rift system, which extends 6500 km from the Jordon to the Dead Sea rift through the red sea, the Gulf of Aden, and the East African rift, according to (Tazieff and Varet, 1972).

During the evolution of the Afar, periods of stronger and weaker tectonic and volcanic activities had occurred. However, there have also been periods of no volcanic and tectonic activities for which Afar did not have an evolution of uniform continuity but rather have showed increased tectonic and volcanic activities. According to (Mohr and Wood, 1976; Ebinger and Casey, 2001), the tectonic evolution of Afar shows the following activities:

- Continuous faulting during the deposition of the volcanic units over lacustrine sediments
- Period of tectonisim and volcanism
- Deposition of sediments in grabens

D. Research Objective
a) General Objective

The general objective of this research was mapping lithology and structures using remote sensing and GIS techniques in the Serdo area, Afar Region, Ethiopian rift valley.

b) The Specific Objectives

- To identify and map the lithology and structures formed in the Serdo area by remote sensing and GIS techniques and methods at a 1:100,000 scale.
- Predicting the tectonic evolution of the area and economically important resources available in that area which includes; mineral deposits and geothermal energy.
- To develop a static geological model commonly used for managing natural resources and natural hazards and quantifying geological processes in the study area
- To produce a system which minimizes risk and safe energy and resource which is lost during fieldwork in

geological investigation especially in the desert and inaccessible area.

II. LITERATURE REVIEW
A. Utility of Digital Image Processing of Multispectral Medium Resolution Data to Geology Applications

According to Kruse (1998), the use of enhanced images, integration of GIS and remote sensing data, and use of narrower spectral bandwidth data has aided geological mapping, an application where the mineralogy, weathering characteristics, and geochemical signatures are useful in determining the nature of rock units, the success of a classification relies on the separability of training data into the various target classes. Thus multispectral and hyperspectral data allowing individual rock types to be studied spectrally and signature or spectral index be obtained have greatly boosted geological investigation. Such studies have explored the utility of band ratios using Landsat and ASTER data owing to their availability. According to (Boettinger *et al.*, 2008; Campbell, 2002, 2009; Chen and Campagna, 2009), Landsat bands are known for particular applications: band 7 (geology band), band 5 (soil and rock discrimination), and band 3 (discrimination of soil from vegetation)). Band ratios are also known for eliminating shadowing and topographic effects and therefore suit complex terrain. The need to normalize band ratios to ease scaling has paved the way for spectral indices while still maximizing the sensitivity of the target features. Examples of band ratios that have been used in geology applications using Landsat are 3/1-iron oxide (Gad and Kusky, 2006), 5/1-magnetite content (Sabins, 1999), 5/7-hydroxyl bearing rock (Sultan *et al.*, 1987), 7/4 - clay minerals (Laake, 2011), 5/4*3/4-metavolcanics (Rajendran *et al.*, 2007).

III. MATERIALS AND METHODS

A. Description of the Study Area

The study area lies in Afar National Regional State in zone 1 at ~700 km from Addis Ababa to Djibouti cross country road in the northeast of Ethiopia. The study area is lying in subtropical climate classified as semi-arid and arid climate zones. The temperature ranges from 26ºC to 36ºC. The temperature commences to increase from April and to reach up to 42ºC in June and July. Rainfall is bi-modal throughout the region, with a mean annual rainfall below 500 mm in the semi-arid, decreasing to 150 mm in the arid zones. The region receives rain from (June to September) and two short rainy months December and March to April. The area is characterized as desert scrubland. Vegetations are mostly drought-resistant plants such as small trees, shrubs, and grasses. The geographic location of the study area bounded by latitude $11º 00'00"N−12º 00' 00"$ N and longitude $41º 00' 00"E−42º 00' 0"$ E covering a total area of 12321 km^2 (Fig. 3.1).
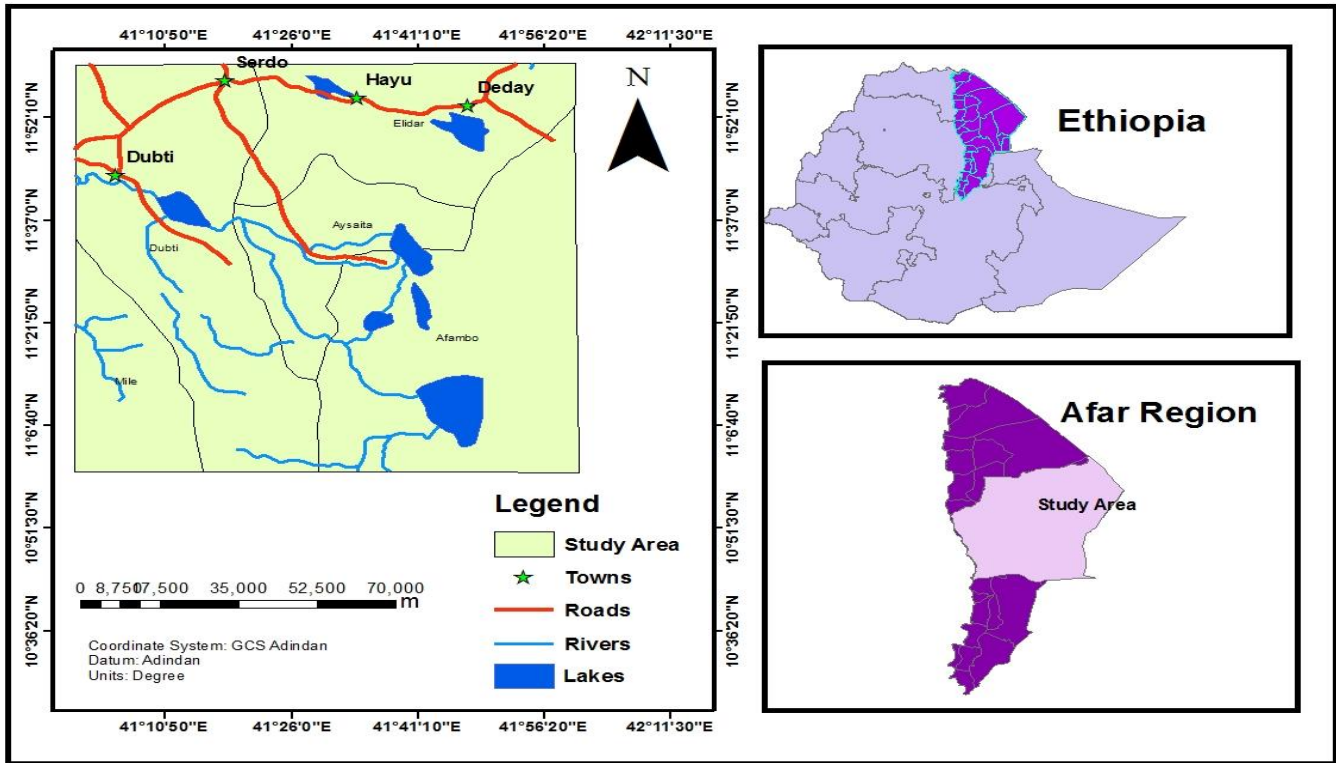
Figure 3.1 Location map of the study area.

B. Materials
a) Data and Software
 Primary task of the present study encompassed gathering of relevant and available data that are essential to accomplish the study objectives, accordingly the following study materials were important for research work.

Earth observation satellites map the physical properties of the earth's surface and near-surface. In the context of geological mapping, we distinguish two types of electromagnetic methods.

Passive optical methods: use the sunlight as the source and measure the reflectance of the earth's surface in the visible and infrared spectral bands. The cloud-free level 1T (terrain corrected) Landsat 8 image of 2015 from the U.S Geological Survey data set was used in this study.

Active microwave radar methods: use a microwave source onboard the satellite and measure the back-scatter from the earth. Digital elevation model, DEM 30 m from the Shuttle Radar Topographic Mission (SRTM) data were used in this study.

Landsat 8 satellite image from U.S Geological Survey data set, digital elevation model DEM (Shuttle Radar Topography Mission SRTM) 30 m from U.S Geological Survey data set to provides terrain relief and facilitate identification of geological structures, existing published geological map covering the research study area (1:250,000) from Ethiopian Geological Survey, published topographic map covering the research study area (1:50,000) from Ethiopian Mapping Agency this forms the geographic base map of the area and is essential for geo-referencing, measuring tape (meter), compass, geologic hammer, sample bag, digital camera, GPS (global positioning system) laptop (preferable), software such as Microsoft Office2007, ERDAS Imagine 2014, ArcGIS10, Surfer11(for contouring, gridding, and 3D surface mapping) and Global Mapper.

C. Methodology
The methodology involved the collection of primary data, which includes spatial data such as Landsat 8 satellite image, DEM data, and non-spatial data such as field data, different map sheets, and measurements surface rendered DEM data 3Dmodel, hills hade, surface derived attributes slope, aspect, curvature from secondary data previous works and reports. After data collection, image preprocessing techniques applied, data analysis and synthesis (False-color composite (FCC), True color composite (TCC), convolution, principal component analysis (PCA), and intensity hue saturation transformation(IHS), then a field investigation in some selected test areas in order to validate the accuracy of the visual interpretation. The detailed framework of the study was presented in (Fig.3.3).
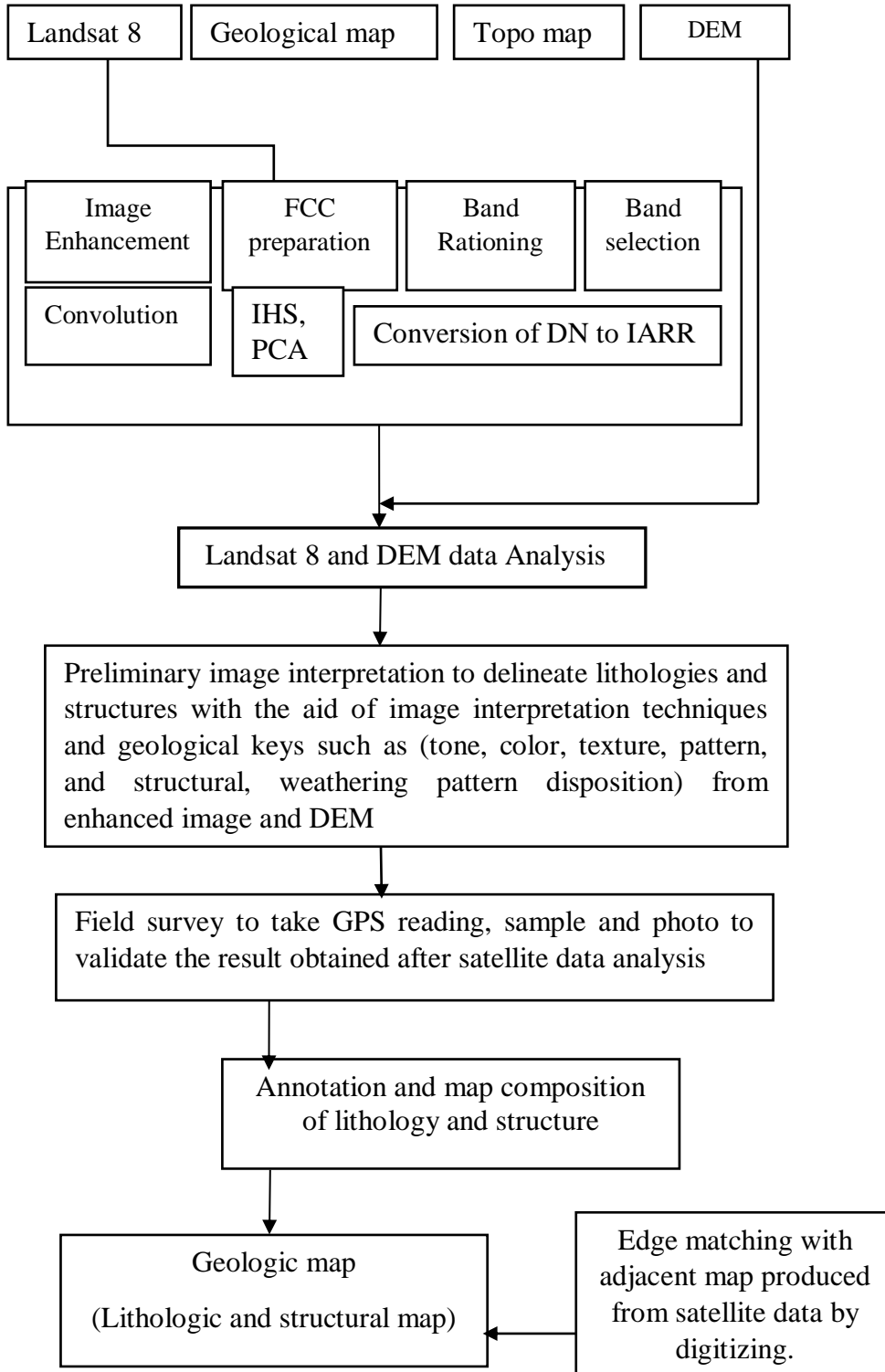
Figure 3.3 Methodological flowchart

To achieve the general and specific objectives, the following methods and approaches have been followed.

D. Pre-Field Work

The activities that are conducted during pre- fieldwork were:

Relevant data such as a topographic map and geological map were collected and analyzed, the project area from the topographic map was delineated.

Shuttle radar topographic mission DEM data and landsat8 satellite images of Entity ID: LC81670522015206LGN00 Coordinates: 11.56789, 41.42345 Acquisition Date: 25-JUL-15

Path: 167

Row: 052 were downloaded and preprocessed.

The major geological structures and lithological contacts based on the DEM data from preprocessed SRTM and satellite image of Landsat 8 were identified and located visually.

a) Applications of Geographic Information System
In this study, GIS was primarily applied for the purpose of data integration, visualization, and cartographic work, and for data analysis.

b) Processing of Landsat 8 OLI/ TIRS Data
Landsat 8 data were converted to surface reflectance using the Internal Average Relative Reflectance according to (IARR) method (Ben-Dor *et al*., 1994). Ben-Dor *et al*. (1994) recommended the IARR reflectance technique for mineralogical mapping as a preferred calibration technique, which does not require prior knowledge of samples collected from the field. During the atmospheric correction, raw radiance data from imaging spectrometer is re-scaled to reflectance data. Therefore, all spectral are shifted to nearly the same albedo. The resultant spectral can be compared with the reflectance spectral of the laboratory or field spectra directly.

The full subset Landsat 8 bands were imported in the geographic coordinate system. The imported images were path-oriented. In order to transform the to north-up UTM, the images were re-projected using the following parameters: UTM Projection, Adindan UTM zone 37N, and Nearest Neighbor re-sampling method. The study area lies in Grid UTM zone 37. The Landsat 8 spectral subset bands have different spatial resolutions. The coastal/aerosol, visible and near-infrared (VNIR), SWIR-1 SWIR-2, bands 1, 2, 3,4,5,6

and 7 are 30 m resolution. The thermal inferred (TIR-1, TIR-2) bands 10 and 11are provide in 100m resolution, Cirrus band (9) 30 m and Pan band (8)15 m. The Visible, NIR, and SWIR bands are merged to panchromatic 15 m resolution to attain a consistent resolution for subsequent processing. The panchromatic and cirrus cloud (band 9) bands and thermal inferred (TIR-1) band 10 are supplementary tools in this study (Table 3.1) shows Landsat 8 OLI and TIRS Bands characteristics.

Table 3.1 Landsat 8 OLI and TIRS Bands characteristics.

Spatial resolutions and subsystems	Spectral range(μm)	Bands
30 m Coastal/Aerosol	0.435−0.451	Band 1
30 m Blue	0.452−0.512	Band 2
30 m Green	0.533−0.590	Band 3
30 m Red	0.636−0.673	Band 4
30 m NIR	0.851−0.879	Band 5
30 m SWIR-1	.566−1.651	Band 6
100 m TIR-1	10.60−11.19	Band 10
100 m TIR-2	11.50−12.51	Band 11
30 m SWIR-2	2.107−2.294	Band 7
15 m Pan	0.503−0.676	Band 8
30 m Cirrus	1.363−1.384	Band 9

1) Band Selection
For the purpose of image display, only three bands or band combinations, each directed to one of the primary color-gun (Red, Green, and Blue), are required. In order to enhance the desired target and avoiding the redundancy of information, spectral bands having the most information contents should be selected. Different workers demonstrate the possibility to select band combinations that contain the highest possible amount of information using a statistical approach. In this study, the optimum index factor (OIF) method introduced by Chavez *et al*. (1982) was adapted. The Optimum Index Factor (OIF) is a statistical calculation of every possible 3 band combination, based on total variance within bands and correlation coefficient between bands.

The index given by:

$$OIF = \sum_{i=1}^{3} SDi \,/\, \sum_{i=1}^{3} ABC(CCj) \qquad eq\,(1)$$

Where SDi is the standard deviation of the band, i and ABC (CC j) is the correlation coefficient between any two of the possible three pairs. The highest value of OIF should be the three bands having the most information content (Chavez *et al.,*(1982).

Various band combinations were visually inspected to support the statistical method, and most of the high-rank band combinations give helpful geological information. The band combination 7, 4, and 3 with the lowest OIF at a rank number of higher values provide good color contrast between different lithologic units and structures also apparently enhanced (band 5.4 and 3) for Landsat 8 in this work.

2) Haze Correction
Space-born optical sensors recording data in the visible and shortwave inferred spectrum receive solar radiation reflected from the Earth's surface and radiation scattered by the atmosphere. Since the atmospheric effect due to haze, aerosol, and etc., modifies the radiation reflected at the ground, reducing image contrast, and contributes an additive term, correction is necessary in order to convert the "at sensor" or "top-of-atmosphere" radiance to ground, leaving radiance. To determine the portion of the at-sensor or radiance that is attributable to ground properties, while subtracting out the portion that is attributable to atmospheric effects in the situation when actual atmospheric data are not available is done by "dark object subtraction" approach given by (Crane, 1971). The method is based on the assumption that the atmospheric scattering throughout the scene is uniform, and somewhere in the image, there is a pixel with zero reflectance, such that the radiometric contribution from this pixel represents only the additive term.

3) Image Enhancements
Landsat 8 data were digitally processed, and several spatial and spectral enhancement techniques, namely: contrast stretching, HIS transformation, principal component analysis (PCA), band rationing, and spatial filtering, were applied. The enhancement gave substantial results in geological interpretation is briefly summarized in the following section.

4) Linear Contrast Enhancement
Contrast enhancement is one of the most widely used image processing techniques for geological studies. It is the process of redistributing the brightness levels in an image to utilize the entire dynamic range of the display device. In order to produce an enhanced image during data processing, the raw data stretch over the quantized range of grey value (256 for 16-bit data). The resulting enhancement, however, is strongly controlled by mean and standard deviation statistics of the input data and consequently influences the resulting color in image composites since they regulate the brightness of the bands under consideration and thus the corresponding colors.

For this study, the stretched images have been interpreted for lithologic and structures interpretation.

5) Intensity Hue Saturation Transformation
According to (Sabins,1987) Intensity Hue Saturation (IHS) transformation is a process in which a band's Red Green Blue composite is decomposed into intensity (I), hue (H), and saturation (S) components, and after manipulated then it is transformed back to the RGB space for interpretation. Intensity represents the brightness, hue signifies the dominant wavelength, and saturation is related to the purity of a color (Sabins, 1987). The advantage of this technique is its ability to effectively separate intensity and spectral information from the standard image and the possibility to convert IHS elements back to RGB space. The resulting enhanced color images are easier to interpret as the spectral information. (Hue) is not changed during transformation.

6) Principal Component Analysis
The principal component analysis (PCA) transformation is a multivariate statistical method used to compress multispectral dataset into few PC images in which spectral difference between materials become apparent in PC image than individual bands (Sabins, 1987; Gillespie *et al*., 1986). Principal components are commonly calculated using the covariance matrix obtained from the multispectral input data, whereby the corresponding eigenmatrices are also determined. In this study, PCA was performed on landsat8 data covering the 7 bands (Visible, NIR, and SWIR). For lithologic discrimination and the color composite created from the PC, images give valuable geological information.

7) Band Rationing
To evaluate the Landsat 8 data, different Red Green Blue color combination images, band ratios were applied for enhancing the lithologic units. Band rationing is a technique where the digital number value of one band is divided by the digital number value of another band. Band ratios are very useful for highlighting certain features or materials that cannot be seen in the raw bands (Inzana *et al*., 2003, Pour *et al*., 2013, 2014).

This procedure involves the division of two bands, where the band with high reflectance features of the given material is assigned as the numerator, while the other band with high absorption feature for the same material is assigned as a denominator. Rationing can be thought of as a method of enhancing minor differences between materials by defining the slope of the spectral curve between two bands. The resultant gray-scale band ratio image is not a direct measurement for the material's contents, and rather it marks the area with the highest possibilities for the presence of the given material. The combination of three-band ratio images as red-green-blue (RGB) images is useful for the interpretation of the result. Band rationing and combinations with most contrast were also investigated using Drury, (1993) principle whereby, for bands ratios involving geology, a higher band is divided by a lower band. From algebra combinations and permutations, bands (4, 6, and7) as the numerator for Landsat 8. Thus combinations (4/3, 6/2,

7/3) were found to have the best contrast, and they formed the input for classification.

8) Spatial Enhancements

One of the characteristic features of the satellite images is a parameter called spatial frequency, which is defined as the number of changes in brightness value per unit distance for any particular part of an image. According to (Jensen 1996), if there are very few changes in brightness value over a given area in an image, this is referred to as a low-frequency area. Conversely, if the brightness values change dramatically over a short distance, this is an area of high frequency. Spatial filters emphasize or deemphasize image data of variable frequencies that refer to the roughness of the total variation (Lillesand *et al*., 2004). The process involves matrix operations where the spatial distribution of the pixel and the moving window size play an influential role. Filters that operate in the frequency domain are implemented through the Fourier transformation, whereas those which operate in the spatial domain of the image itself are known as convolution filters (List, 1993).

9) Processing of Digital Elevation Model

Compared to two-dimensional satellite data, a Digital Elevation Model (DEM) has the advantage of representing the vertical extension of the earth's surface by assigning height values for every pixel. The use of DEM has a marked interest for geological mapping, especially for highly vegetated terrains and urban areas.

A C-band system (5.6 cm wavelength; C-RADAR) and an X-band system (3.1 cm wavelength; X-RADAR) 30 m resolution of Shuttle Topographic Mission Radar (SRTM) are downloaded from USGS, and geometric correction, as well as speckle reduction (despeckle) processing, applied. The operational goal of C-RADAR is to generate contiguous mapping coverage as called for by the mission objectives. X-RADAR generated data along discrete swaths 50 km wide. These swaths offered nearly continuous coverage at higher latitudes.

Several processed Digital Elevation Model (DEM) products, such as the hill-shading, painted shaded-relief, maps of slope and aspect, have been processed for the identification of geological structures. In this study, spatial enhancement is mainly applied to facilitate visual interpretation of image and DEM data for the purpose of structural mapping using convolution filters. For the identification of the smaller and medium-sized structure, the mid-low filters of 3x3 window edge detection filters known as Gradient-Soble and Gradient-Prewitt were utilized, and for the larger structures, 7x7 window size directional filters were used, adapted from Kenea (1997).

c) Field Work

Various data types are collected during fieldwork: One field visit with a total of 15 days was conducted during 1−16 December 2015 for verification of the preliminary interpretation results. Due to the inaccessibility and hot climate of the study area, only the north and northeast parts were visited. Global positioning system (GPS), topographic maps (1:50,000 scale), digital camera, and interpreted maps resulted from satellite image were used. The global position of field observation points and collected samples note on observations were recorded.

d) Post Field Work

- Field information was compiled in GIS software to show generated geological map, which shows lithological units, major geological features, and structures.
- Finally, by integrating the pre-field, during the field, and post-field works, a hardcopy of the large-scale geological map of the study area with a scale of 1:100,000 and static geological model was produced.

E. Image Interpretation

Visual image interpretation is carried out by geologist perception, spontaneous recognition, and logical inference (reasoning by professional knowledge) of the researcher. The interpretation of lithology and structure was performed by applying image interpretation keys, such as color (tone), texture, shapes, patterns, and interrelationship between features that may have geological significance. From processed Landsat 8 images, volcanic rocks such as lava, Rhyolites, and vesicular basalts are clearly identified by their pattern or grey color, alluvial deposit and sediments are also clearly identified by their tonnage or brown color. Data from field visits were utilized for image interpretation and verification of results obtained from digital image processing. The enhanced true-color composite image provides a good overview of the study area in a color composite that is most familiar and close to natural

F. Lineaments Interpretation

In order to understand the geological significance of structures and ease of data interpretation, the geological structures are grouped into parts based on the relative homogeneity of measured linear features. The presence of a common regional fault and graben system has pictured the specific physiography of the study area. These faults and graben systems are categorized according to their size extent.

a) The Tendaho Graben

The graben is an elongated block of earth's crust lying between two faults and displaced downwards, as in a rift valley.

The Tendaho graben is one of the major structures identified in the area trending in the NW direction and larger throw observed on the east bounding faults. This graben is floored by alluvial deposits, newly emerging land features, and recent volcanic craters and domes. Open fissures, fractures, and NW striking active normal faults were also observed at the floor of the rift, some of which were diffused into the scoria cones.

1) The Axial Grabens

The orientation this (around east of Gumarre lake, Dobi, and Guma) grabens trend is NW and expressed as a complex zone of escarpments consisting of faults that seemed to be rotated. These grabens are floored by alluvial sediments and evaporate. Whereas the fault ground was covered by aphanetic and vesicular basalts. During fieldwork, the attitude of bedding, fractures, and dyke orientation is checked. The field observation also witnesses those major structures' orientation coincides with the direction of NW faults strike.

2) Volcanic Calderas

These geologic features are relatively the youngest features seen in the study area from morphology structures because they exhibit undisturbed appearance. According to visual interpretation, four volcanic calderas are identified. These are the Kurub volcano at the north, Demalle volcano, and Gabillema volcano at the south. In addition to the above-mentioned geologic features, water bodies and vegetated areas are also identified by image interpretation techniques (Fig 3.6) shows the visually interpreted major geological features in the study area.

IV. RESULTS

A. Enhanced False Color Composite

Lithologic and structural information is generally well contained in many of the high-ranking band combinations. Band composite (5, 4, 3) and (7,4,3) in RG B contains the maximum information was given in (Fig.4.1). The contrast between the different lithologic units was also apparently enhanced in-band composite7,5 and 3 in RGB, selected by visual inspection of various band composite possible from landsat8 VNIR and SWIR data.
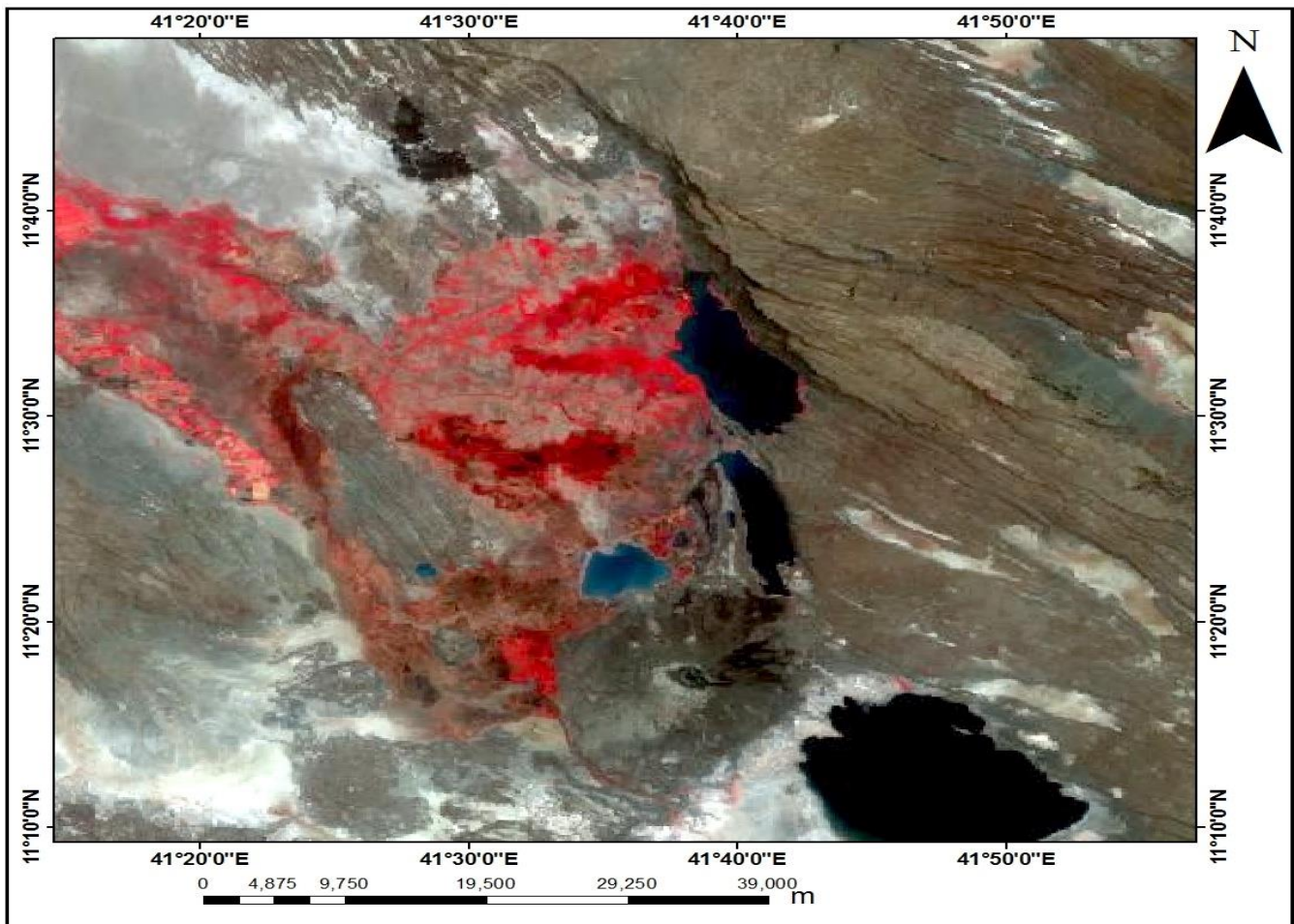
Figure 4.1 Enhanced False-color composite from Landsat 8 bands of (5, 4, 3) in RGB.

a) Intensity Hue Saturation Transformation

The intensity and spectral information of lithologies were effectively separated from that of the standard image by intensity hue saturation transformation. Figure 4.2 shows intensity hue saturation transformed image of the study area.
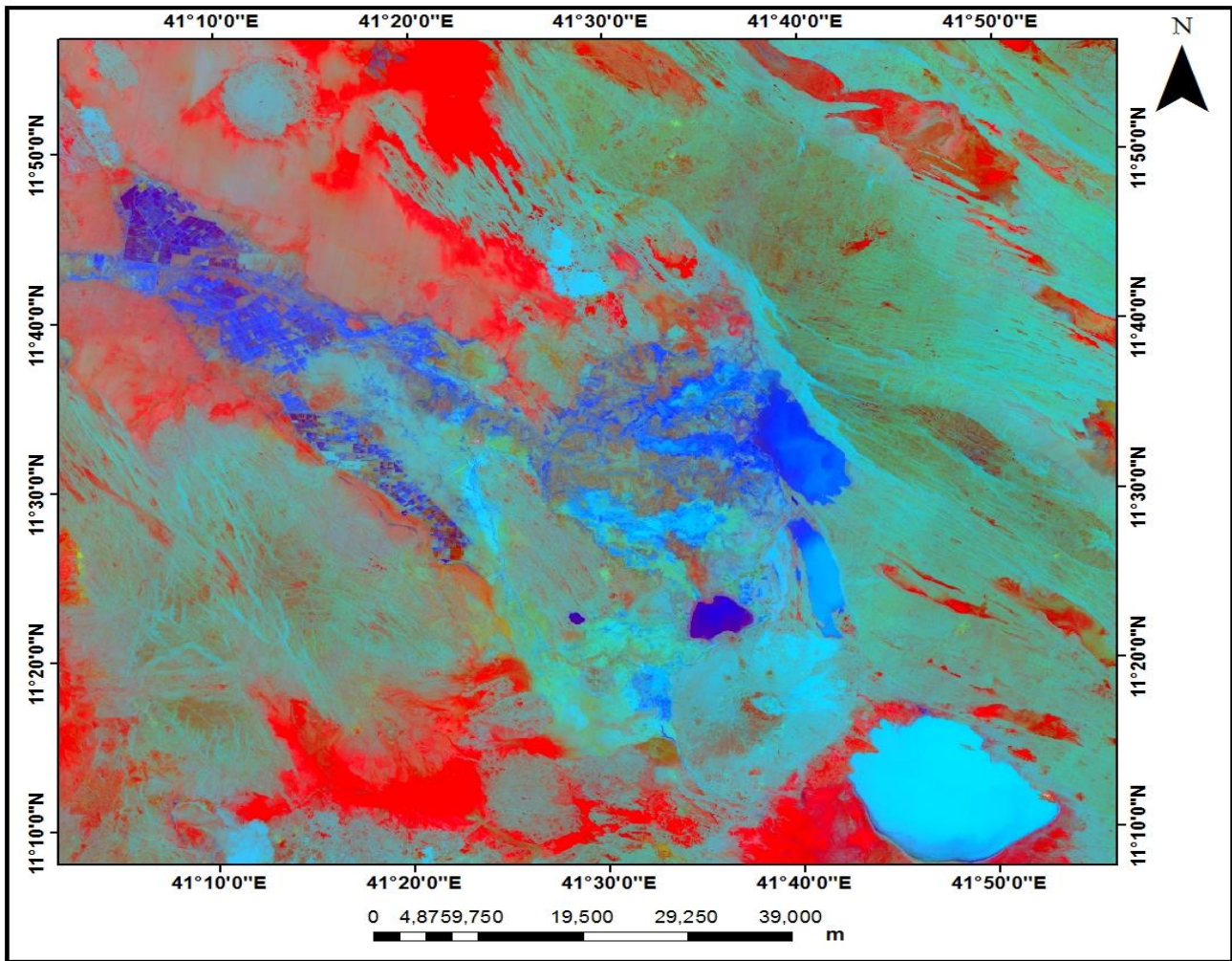
Figure 4.2 Intensity hue saturation transformed the image of the study area.

b) Principal Component Analysis

PCA was performed on seven (7) bands. Compressed redundant data values into bands, which are often more interpretable than the source data, were shown by PCA. This compresses multispectral dataset into few PC images in which spectral difference between materials become apparent in PC image than individual bands. The eigenvector and eigenvalue statistics used for the transformation of Landsat 8 OLI (7 bands) was showing in Table 4.1.

Table 4.1 Eigenvector and eigenvalue statistics for landsat 8 OLI (7 bands).

Eigenvector	PC1	PC2	PC3	PC4	PC5	PC6	PC7
Band1	0.1556	-0.1458	0.2888	0.5145	-0.1035	-0.3492	0.6882
Band2	0.2041	-0.1762	0.3519	0.4898	-0.1335	-0.1898	0.7138
Band3	0.2882	-0.1948	0.4194	-0.0058	-0.0361	0.8279	-0.1278
Band4	0.3888	-0.3335	0.3558	0.6776	0.01827	-0.3892	-0.0040
Band5	0.4922	0.8244	0.1695	-0.0021	0.2155	-0.0533	0.0039
Band6	0.5076	-0.0144	-0.5023	0.0080	-0.6983	0.0417	-0.0151
Band7	0.4470	-0.3445	-0.4572	-0.1897	0.6600	0.0243	.0124
Eigenvalue	1759.03	1367.06	7124.2	425.4	307.58	44.40	6.44

PC1, with positive loading from all Landsat 8 bands, contains significant albedo and topographic information, and that accounts for a high correlation between the input bands. PC1, PC3, PC4, and PC5 display fair lithologic contrast, and the rest of the PC (PC2, PC5, and PC7) show noisy images and appear to be less informative. RGB composite of PC1, PC3, and PC4 have better color contrast and allowed the best lithologic discrimination. Figure 4.3 showing the Landsat 8 PC1 image of the study area.
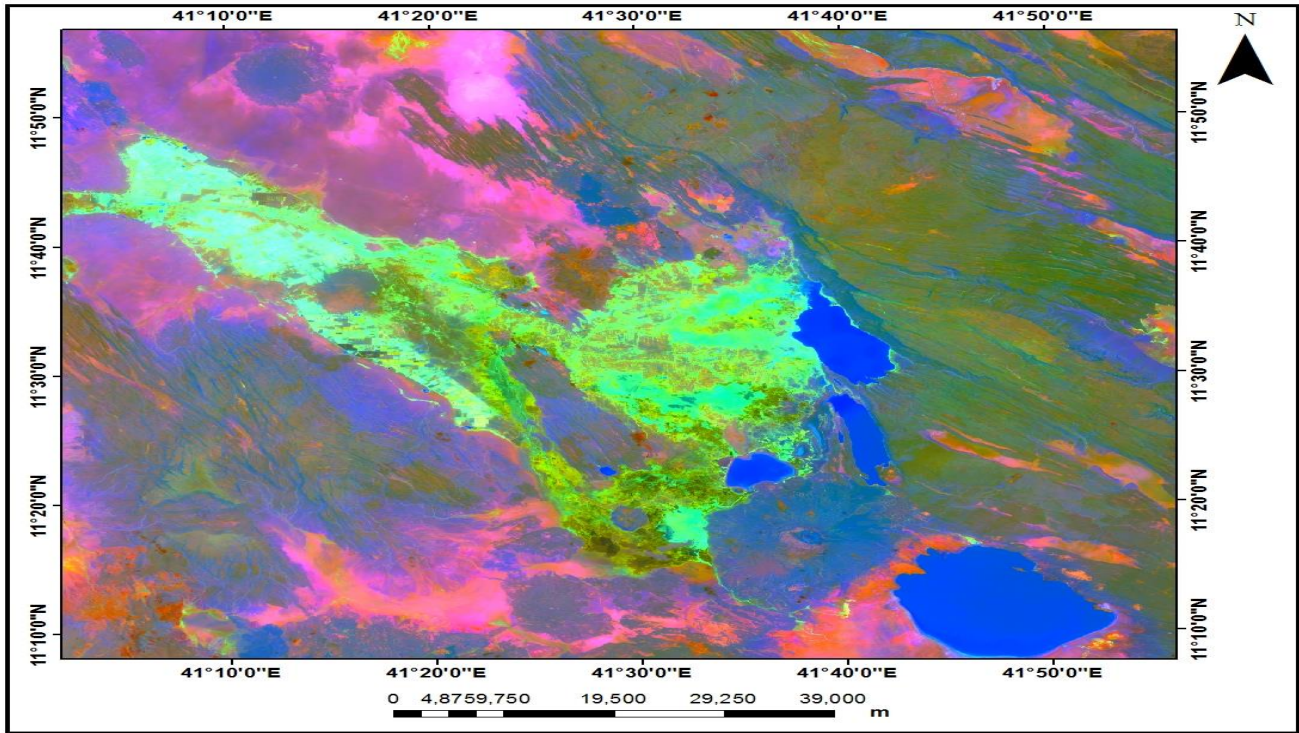
Figure 4.3 Landsat 8 OLI Principal Component Analyses (PC1) Map.
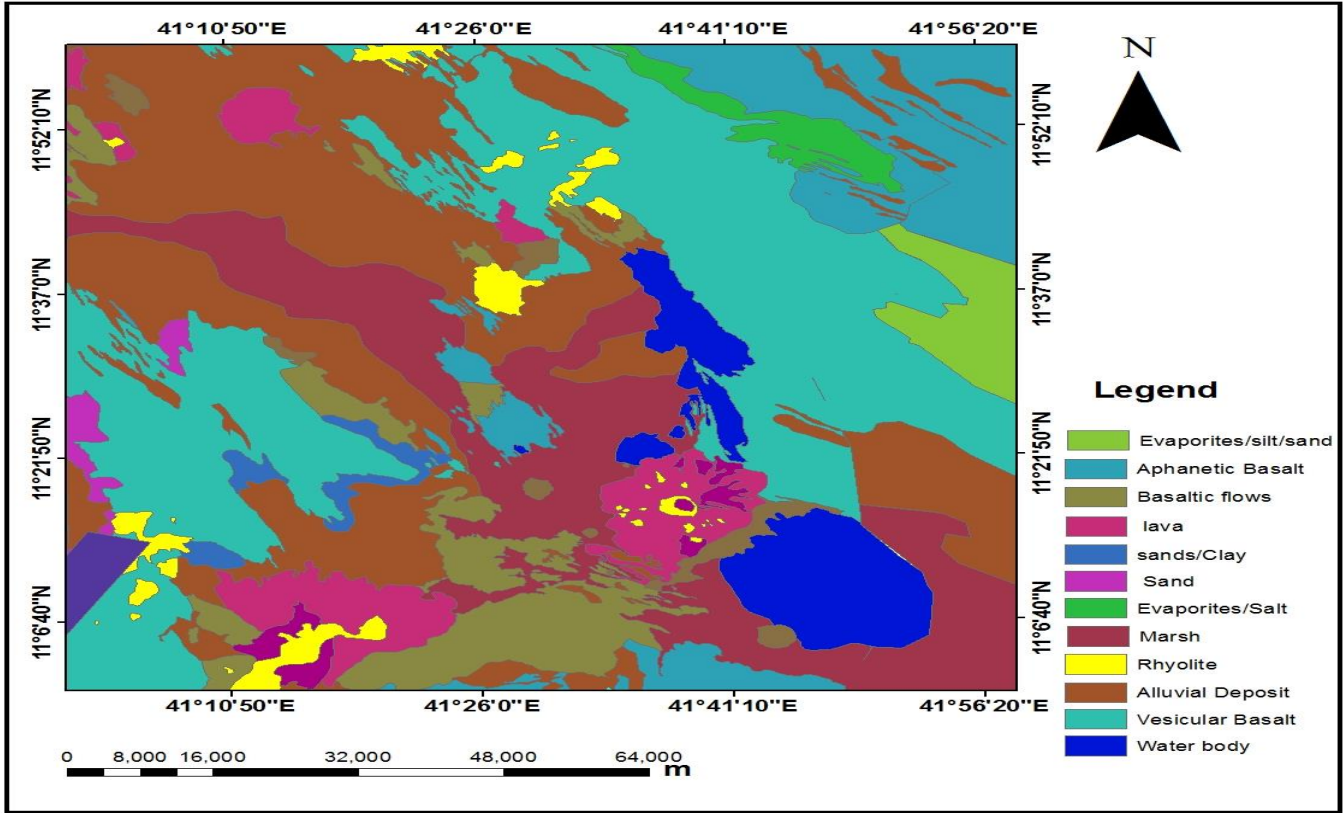
Figure 4.4 Interpreted lithology map of the study area.

B. Convolution Filtering

Across the study area, the superposition of a different set of brittle structures was identified in all mapped volcanic formations (e. g. normal regional faults to oblique-slip faults, shear joints, and extensional joints). Spatial enhancements were performed using directional filters for the purpose of lineament and structure analyses. Directional filters were selected for producing effects that may reveal tectonically controlled planar and linear features

a) Gradient-Soble and Gradient-Prewitt Mid-Low Filters of 3×3 Window Size Edge Detection

Total 1651minor lineaments are identified in the study area. Table 4.2.and Figure 4.5 showing minor lineaments detected from gradient-soble and gradient-prewitt mid-low filters of 3×3 window size edge detection.

Table 4.2 Filter 3×3 window size edge detection applied.

Soble edge detection 3×3 filter			
	-1.000	-1.000	-1.000
	-1.000	**8.000**	-1.000
horizontally	-1.000	-1.000	-1.000
vertically	-1.000	-1.000	-1.000
	2.000	**2.000**	2.000
	-1.000	-1.000	-1.000
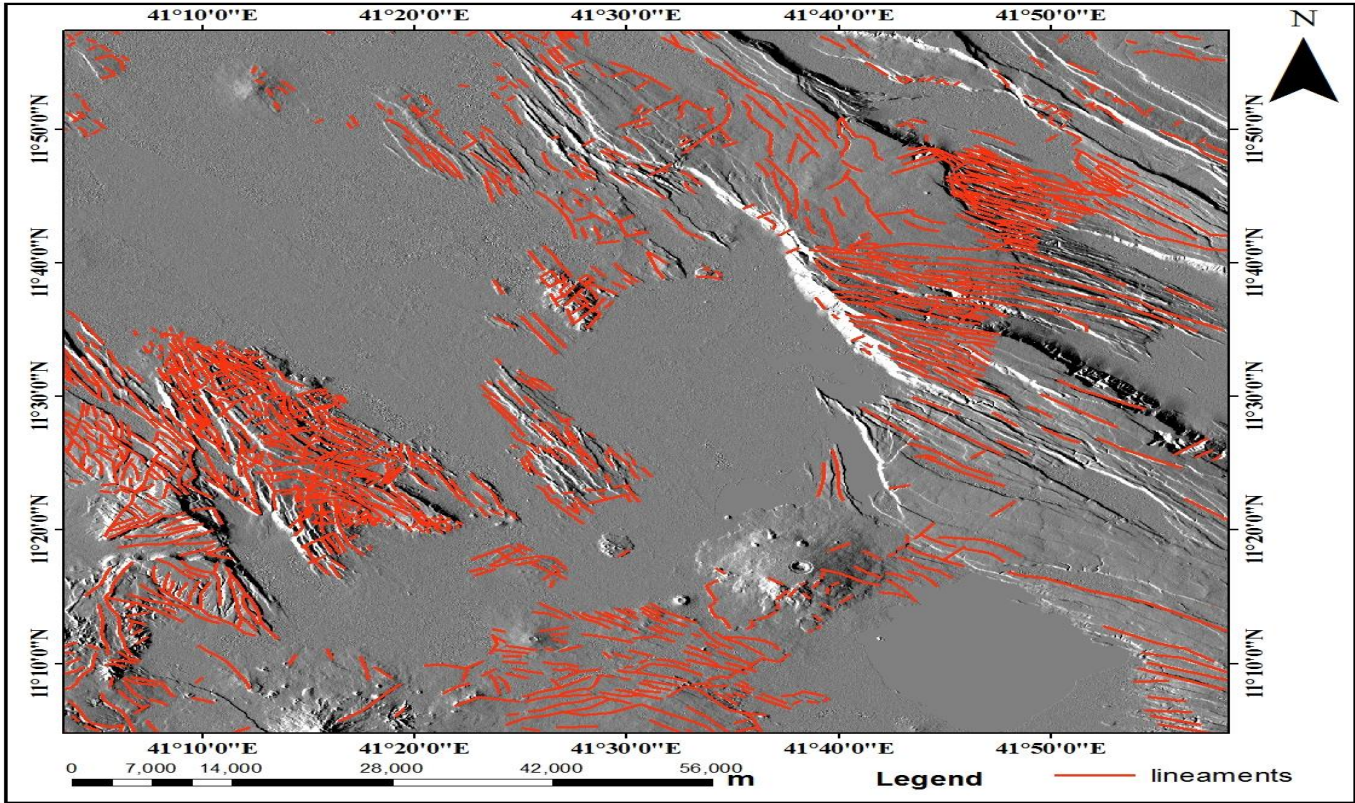
Figure 4.5 Minor lineaments detected from 3×3 window size of edge detection

b) Window Size Directional Filters of 7×7

The major regional faults of the area are the graben bounding faults, which are characterized by the high angle with extensive length and throw. Their strikes have actually determined the direction of most of the grabens of the area, with NW as a dominant strike direction. These faults have a high throw greater than around 350−400 m east dawn throw and west dawn throw. Totally 56 major faults are identified (Table 4.3 and Fig 4.6) show major faults identified by 7×7 window size directional filters.

Table 4.3 7×7 Window Size Directional Filters applied North-South direction.

7×7 Window Size Directional Filters	
North-South	-1.000-1.000-1.000-1.000-1.000-1.000-1.000 -1.000-2.000-2.000-2.000-2.000-2.000-1.000 -1.000-2.000-3.000-3.000-3.000-2.000-1.000 -1.000-2.000-3.000 **80.000**-3.000-2.000-1.000 -1.000-2.000-3.000-3.000-3.000-2.000-1.000 -1.000-2.000-2.000-2.000-2.000-2.000-1.000 -1.000-1.000-1.000-1.000-1.000-1.000-1.000
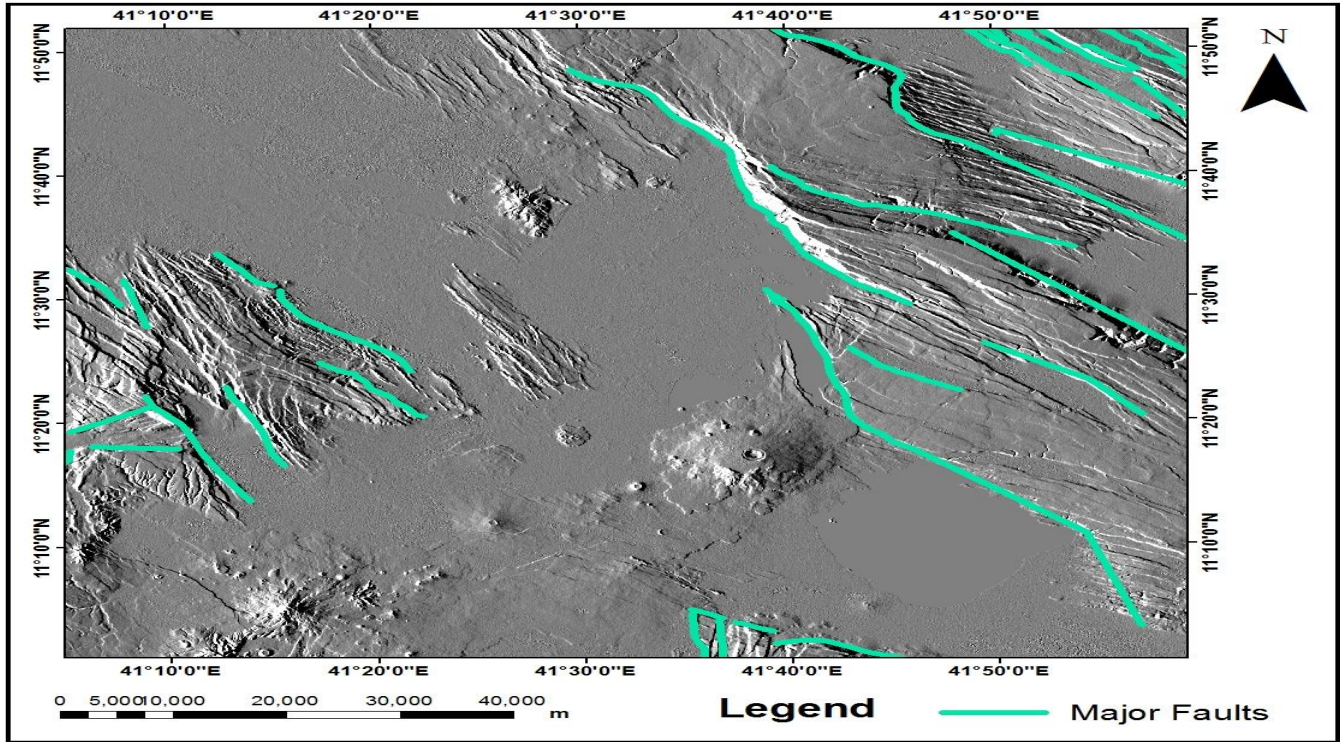
Figure 4.6 Major faults detected from 7×7 window size directional filters.

The finalized structural map is presented in (Fig.4.7) by the integration of 3×3 window size edge detection,7×7 window size directional filters, aspect map, and painted and relief map.
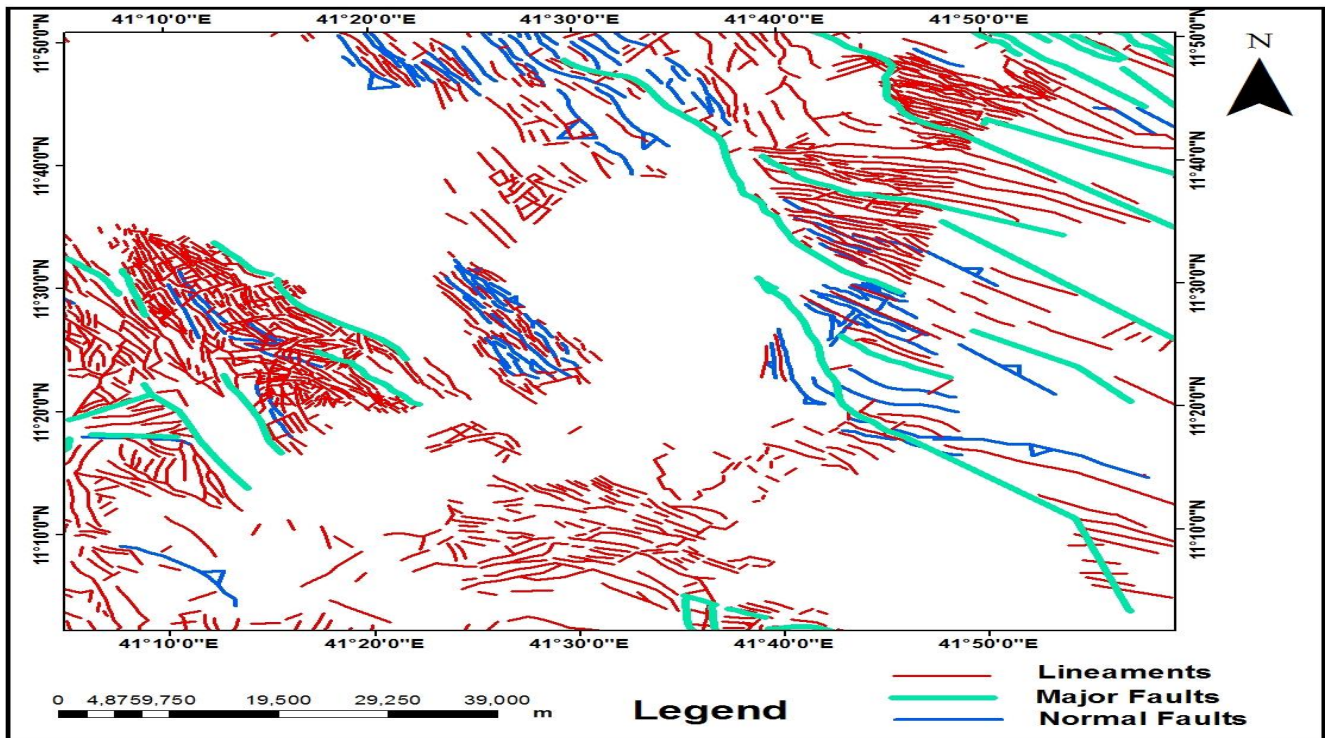
. **Figure4.7 Detailed and generalized interpreted structure map of the study area.**

V. CONCLUSION AND RECOMMENDATIONS

A. Conclusion

Using Landsat 8 data combined with DEM is an effective tool for lithologic and structure detection. Analyzing of Landsat 8 OLI/TIRS and Digital Elevation Model data covering the study area have shown.

➢ The effectiveness of applying Landsat 8 OLI/TIRS data for geological mapping through the identification and interpretation of subtle spectral and spatial information difference between different lithologic units.

➢ The study illustrated the use of Landsat 8 and remote sensing data and edge enhancement techniques for lithologic mapping and the applicability of Shuttle Radar Topographic Mission DEM data for geological mapping structures on the basis of their geomorphologic expression.

➢ The investigation also demonstrates significant implications for geologists to utilize Landsat 8 OLI/TIRS data for geological purposes in the future.

The overall result of this study demonstrates that the Landsat 8 OLI/TIRS and Digital Elevation Model data set can be used as an effective tool for lithological and structural mapping. Although lithological and structural mapping using the satellite remote sensing technique is somewhat hindered by the presence of vegetation cover and the spectral similarities between some of the lithological units caused by the similar vegetation cover, a lithological map with Internal Average Relative Reflectance and structural map with DEM is satisfactory. Therefore, Landsat 8 OLI/TIRS and Digital Elevation Model data can be used to increase lithological and structural discrimination and enhance the overall mapping performance, and to define for any investigation such as weak zone detection for groundwater and engineering geology, targets for mineral exploration, particularly in the area of good rock exposure (minor soil development and small or absence of vegetation).

B. Recommendations

Based on the experience I gained from this study and the review of different journal articles, I would like to recommend the following point.

❖ To explore the more detailed surface and subsurface geological information in the study area, it is better to use or apply hyperspectral remote sensing data.

❖ From observed lithologic properties and abundance of structures, the study area is enriched by the following resources: from the alluvial deposit and vesicular basalt groundwater, from alluvial sediments fertile soil for agricultural activities, from major consecutive normal faults, geothermal energy sources, and hydrothermally altered mineral zones and from evaporates table salt.

❖ Earthquake is common along this line. Seismic stations are important in this area to regulate earthquake phenomena.
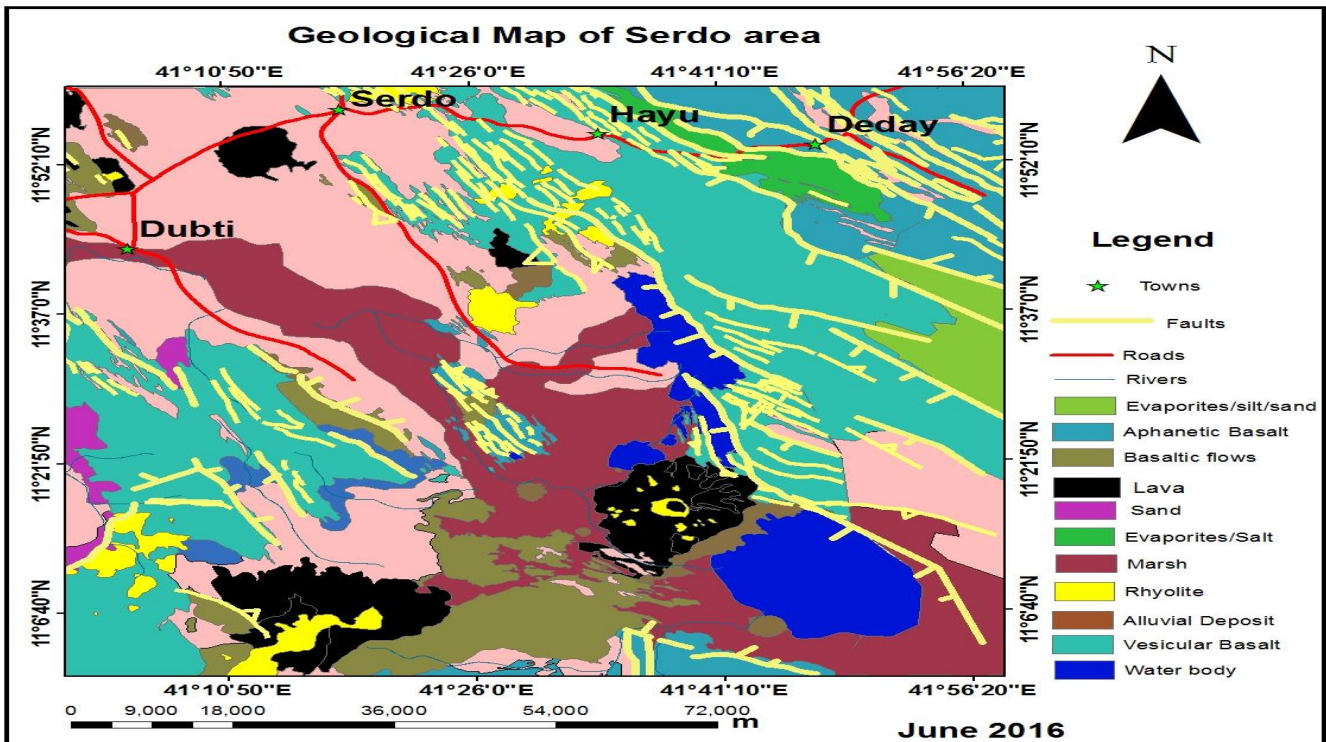
Finalized geological map of Serdo area

References

[1] Abrams, M.J., Rothery, D.A., and Pontual, A., Mapping in the Oman ophiolite using enhanced Landsat Thematic Mapper images.Tectonophysics, 151(1988) 3874–01.

[2] Acocella, V., Tesfaye. K, and F.Salvini, Formation of normal faults along the axial zone of the Ethiopian Rift, J. Structural. Geol., 25(2003) 503–513.

[3] Alwash, M. A.and Zigler, J., Remote sensing-based geological mapping of the area west of AlMadinah, Saudi Arabia, International Journal of Remote Sensing, 15(1)(1994) 163–172**.**

[4] Boettinger, J.L., Ramsey, R.D., Bodily, J.M., Cole, N.J., Kienast-Brown, S., Nield, S.J., Saunders, A.M., and Stum, A.K., Landsat Spectral Data for Digital Soil Mapping. In Digital Soil Mapping with Limited Data, A.E. Hartemink, A. McBratney, and M. de L. Mendonça-Santos, eds. (Dordrecht: Springer Netherlands), (2008) 193–202.

[5] Campbell, J.B., Band ratios. An Introduction to Remote Sensing, (New York: Guilford Press), (2002) 505.

[6] Campbell, J.B., Remote sensing of Soils. In The Sage Handbook of Remote Sensing,(Thousand Oaks, CA: Sage), (2009) 341–354.

[7] Chavez, P. S., Berlin, G.L., and Sowers, L.B., Statistical method for selecting Landsat MSS ratios.Journal of Applied Photograph Eng., 8(1982) 23–30.

[8] Crane, R. B., Processing techniques to reduce atmospheric and sensor variability in multispectral scanner data. Proceeding 7th International symposium Remote Sensing and Environment, 2(1971) 1345–1355.

[9] Chen, X., and Campagna, D.J., Remote Sensing of Geology. In The Sage Handbook of Remote Sensing, (Thousand Oaks, CA: Sage), (2009) 328–340.

[10] Drury, S, A., Image Interpretation in Geology, 66-148 (Kluwer Academic Publishers) 296(1987).

[11] Drury, S.A., Image interpretation in geology (London; New York: Chapman & Hall).,(1993).

[12] Ebinger, C.J., Yemane, T., Wolde Gabriel, G., Aronson, J.L., and Walter, R.C., Late Eocene Recent volcanism and faulting in the southern main Ethiopian rift: Geological Society (London) Journal, 150(1993) 99–108.

[13] Ebinger, C. J., and Hayward, N., J., Soft plates and hot spots: Views from Afar, J. Geophys. Res., 101(1996) 21,859–21,876.

[14] Ebinger, C. J., and M. Casey, Continental break up in magmatic provinces: An Ethiopian example, Geology, 29(2001) 5275–30.

[15] Gillespie, A. R., Kahle, A. B. and Walker, R. E., Color enhancement of highly correlated images, decorrelation and IHS contrast stretches. Remote Sensing Environment, 2(1986) 209–235.

[16] Gad, S., and Kusky, T., Lithological mapping in the Eastern Desert of Egypt, the Barramiya area, using Landsat thematic mapper (TM). J. Afr. Earth Sci.44(2006) 196–202.

[17] Harris, J.R., Eddy, B., Rencz, A., de Kemp, E., Budketwitsch, P., and Peshko, M..Remote sensing as a geological mapping tool in the Arctic: preliminary results from Baffin Island, Nunavut. Current Research 200–1E12, (2001) 13

[18] Inzana, J., Kusky, T., Higgs, G., Tucker, R., Supervised classifications of Landsat TM band ratio images and Landsat TM band ratio image with radar for geological interpretations of central Madagascar. Journal of African Earth Sciences.37(2003) 59–72.

[19] Jensen, J. R., Introductory Digital Image Processing. Prentice-Hall Series in Geographic Information Science, New Jersey, 316(1996).

[20] Kenea, N.H., Improved geological mapping using LandsatTM data, Southern Red Sea Hills, Sudan: PC and HIS decorrelation stretching. Int. J. Remote Sens.18,(1997) 12331–244.

[21] Kruse, A.F., Advances in Hyperspectral Remote Sensing for Geologic Mapping and Exploration In 9th Australasian Remote Sensing Conference, (Sydney, Australia)., (1998).

[22] Laake, A., Integration of satellite imagery, Geology, and geophysical data. In Earth and Environmental Sciences, (INTECH Open Access Publisher), (2011) 467–492

[23] Lillesand, T.M. Kiefer, R.W. and Chipman, J.W., Remote Sensing and Image Interpretation, 5th Ed., John Wiley and Sons Inc. New York, ISBN 0–471–25515–7, 763(2004).

[24] List, F. K., Fundamentals of digital image processing for geological application, Proceeding of the 4th United Nations Ins.Training Course on Remote Sensing Application to Geological Science. Berliner Geowiss Abh. D,5(1993) 7–29.

[25] Mohr, P. A., Surface structure and plate tectonics of Afar, Tectonophysics, 15(1972) 318.

[26] Mohr, P.A. and Wood, C.A., Volcano spacing and lithospheric attenuation in the eastern rift of Kenya. Earth and Planetary Science Letters, 3(1976) 126–144.

[27] Nama, E. E, Lineament detection on Mount Cameroon during the 1999 volcanic eruptions using Landsat ETM International Journal of Remote Sensing, 25(2004) 501–510.

[28] Pour, B. A., Hashim, M, and van Genderen. J., Detection of hydrothermal alteration zones in a tropical region using satellite remote sensing data: Bau goldfield, Sarawak, Malaysia. Ore Geology Reviews. 54(2013) 181–196.

[29] Pour, B. A., Hashim, M, Marghany. M., Exploration of gold mineralization in a tropical region using Earth Observing-1 (EO1) and JERS-1 SAR data: a case study from Bau goldfield, Sarawak, Malaysia. Arabian Journal of Geosciences. 7(2014) 2393–2406.

[30] Rajendran, S., Thirunavukkaraasu, A., Poovalingaganesh, B., Kumar, K.V., and Bhaskaran, G., Discrimination of lowgrade magnetite ores using remote sensing techniques. J. Indian Soc. Remote Sens. 35(2007) 153–162.

[31] Sabins, F. F., Remote Sensing Principles and Interpretation, 2nd ed., (1987) 449.

[32] Sabins, F.F., Remote sensing for mineral exploration. Ore Geol. Rev. 14(1999) 157–183.

[33] Sultan,M., Arvidson, R.E., Sturchio, N.C., and Guinness, E.A. (1987). Lithologic mapping in arid regions with Landsat thematic mapper data: Meatiq dome, Egypt. Geol. Soc. Am. 99(1987) 748.

[34] Tazieff, H., Varet, J., Tectonic significance of the Afar (or Danakil) Depression. Nature 235(1972) 144–147.

[35] Williams, F. M., M. A. J. Williams, and F. Aumento, Tensional fissures and crustal extension rates in the northern part of the Main Ethiopian Rift, J. Afr. Earth Sci., 38(2004) 183–197.